# Vibrational Spectra, DFT Calculations, Unusual Structure, Anomalous $CH_2$ Wagging and Twisting Modes, and Phase-Dependent Conformation of 1,3-Disilacyclobutane

**Mohamed Z. M. Rishard, Richard M. Irwin, and Jaan Laane***

*Department of Chemistry, Texas A&M University, College Station, Texas 77843-3255*

*Received: July 14, 2006; In Final Form: November 29, 2006*

Our previously published infrared and Raman spectra of 1,3-disilacyclobutane (13DSCB) and its 1,1,3,3-$d_4$ isotopomer have been reexamined and partially reassigned on the basis of DFT and ab initio calculations. The calculations confirm previous microwave work that the CSiC angles in the ring are unexpectedly larger than the SiCSi angles. This may arise from the partial charges on the ring atoms. The calculations are in excellent agreement with the observed spectra in both frequency and intensity. They also demonstrate that this molecule has $CH_2$ wagging and twisting vibrations with frequencies below 1000 $cm^{-1}$, about 200 $cm^{-1}$ lower than expected. These unprecedented low values can be explained by the decreased slope in the potential energy curves for these vibrations as the sideways motions of the $CH_2$ groups result in attractive forces between the positively charged hydrogens on the carbon atoms and the negatively charged hydrogens on the silicon atoms. The theoretical calculations also confirm the previous conclusions that the individual molecules (vapor) have $C_{2v}$ symmetry whereas in the solid the molecules become planar with $D_{2h}$ symmetry. The vibrational coupling between the ring-angle bending mode and the $SiH_2$ in-phase rocking, which is present for the $C_{2v}$ structure, is forbidden for $D_{2h}$ and hence disappears.

## Introduction

In 1977 we reported the first synthesis of 1,3-disilacyclobutane (13DSCB) and studied its far-infrared spectra in order to determine its ring-puckering potential energy function.[1] We showed that in the vapor phase, this four-membered ring molecule is puckered with a barrier to planarity of 87 $cm^{-1}$ (0.25 kcal/mol) and a dihedral angle of 24°. Soon afterward, we presented a detailed analysis of the infrared and Raman spectra of 13DSCB in its vapor, liquid, and solid (frozen at 77 K) phases.[2] On the basis of force constant calculations for both $D_{2h}$ (planar) and $C_{2v}$ (puckered) structures and through the observation of vibrational coupling, which changed dramatically upon deuteration of the molecule, we were able to demonstrate that while the molecule has a $C_{2v}$ conformation for the vapor and liquid states, it becomes planar ($D_{2h}$) in the solid. Microwave studies of this molecule[3,4] confirmed the puckered structure for the vapor and also showed unexpectedly large CSiC angles for 13DSCB. In order to confirm our previous assessment of these conclusions, we undertook ab initio and density functional theory (DFT) calculations for 13DSCB and its $d_4$ isotopomer. This has not only allowed us to better understand the structure and the conformational changes and vibrational coupling, but it has also shown us that this molecule has $CH_2$ wagging and twisting modes which have unusually low frequencies. These results will be reported here.

## Experimental

The spectra, which were recorded on a Digilab FTS-20 high-resolution vacuum spectrometer, have been in part previously published[2] and presented in a Ph.D. thesis.[5] Unfortunately, the original journal reproduction of the spectra were extremely faint and difficult to see. Therefore, we will reproduce several of the spectra here and compare these to calculations in this work. To the best of our knowledge, no other laboratory has ever prepared this molecule and hence the only experimental data for 13DSCB come from our earlier work. This is not surprising as the preparation of the molecule is very difficult, involving high-temperature pyrolysis.

## Computations

All of the calculations were done using the Gaussian 03 package.[6] The structures of 13DSCB for its puckered form and its restricted planar form were calculated using the second-order Möller−Plesset perturbation theory with the triple-$\zeta$ basis set (MP2/CC-PVTZ) and also using coupled cluster theory (CCSD) with the 6-311++G(d,p) basis set. DFT calculations were also carried out using six different basis sets, all of which gave similar results for the vibrational frequencies. The calculated frequency values and the computed spectra presented here are from the B3LYP/6-311++G(d,p) basis set. For scaling factors we used 0.964 for frequencies over 1800 $cm^{-1}$ and 0.985 for those below. From previous work[7−10] we have found these factors for this basis set to fit experimental data extremely well (typically within 5 $cm^{-1}$).

**Structures.** The calculated structures of 13DSCB for its $C_{2v}$ (puckered) and $D_{2h}$ (planar) conformations are shown in Figure 1. The puckered structure is the most stable form for non-interacting molecules, and this is calculated to be 160 $cm^{-1}$ lower in energy than the planar molecule. The experimental value is 87 $cm^{-1}$. The computed dihedral angle (Figure 2) is 23.6°, which agrees well with the experimental value[1] of 24°, especially in light of the fact that this is a non-rigid molecule with a large amplitude ring-puckering vibration. Table 1 lists the calculated rotational constants for 13DSCB and its $d_4$ isotopomer, and those for the latter are compared to the experimental microwave values.[3,4] No microwave work was

* Corresponding author.

10.1021/jp064480d CCC: $37.00 
Published on Web 01/18/2007

**TABLE 1: Rotational Constants (GHz) and Structural Parameters of 13DSCB-h$_4$ and 13DSCB-$d_4$**

Rotational Constants

| | 13DSCB-$h_4$ | | | | 13DSCB-$d_4$ | | | | |
|---|---|---|---|---|---|---|---|---|---|
| | MP2/ CC-PVT Z | | B3LYP/ 6-311++ G(D,P) | | MP2/ CC-PVT Z | | B3LYP/ 6-311++ G(D,P) | | experimental[a] |
| | $C_{2v}$ | $D_{2h}$ | $C_{2v}$ | $D_{2h}$ | $C_{2v}$ | $D_{2h}$ | $C_{2v}$ | $D_{2h}$ | $C_{2v}$ |
| A | 7.2227598 | 7.1834176 | 7.1805493 | 7.1748016 | 6.6694736 | 6.6320036 | 6.6280897 | 6.62 18617 | 6.67934814 |
| B | 4.0309313 | 4.0157067 | 3.9619868 | 3.9561814 | 3.3697376 | 3.3496200 | 3.3068958 | 3.30 07636 | 3.39634528 |
| C | 2.9109464 | 2.8360646 | 2.8241468 | 2.8059108 | 2.6265841 | 2.5605183 | 2.5481049 | 2.53 20080 | 2.62452175 |

Parameters (in Angstroms and Deg)

| parameter | MW[b] | DFT[c] | TZ[d] | parameter | MW[e] | DFT[c] | TZ[d] |
|---|---|---|---|---|---|---|---|
| $r_{C-Si}$ | 1.896 | 1.910 | 1.901 | $r_{C-H}$ | 1.09 | 1.090 | 1.092 |
| $\alpha_{CSiC}$ | 92.3 | 91.2 | 90.2 | $r_{Si-H}$ | 1.48 | 1.488 | 1.482 |
| $\alpha_{HSiH}$ | 108.3 | 108.6 | 108.8 | $\alpha_{HCH}$ | 109.0 | 108.1 | 108.9 |

[a] Ref 4. [b] Microwave (calculated); ref 4. [c] B3LYP/6-311++G(d,p). [d] MP2/CC-PVTZ. [e] Microwave (assumed); ref 4.

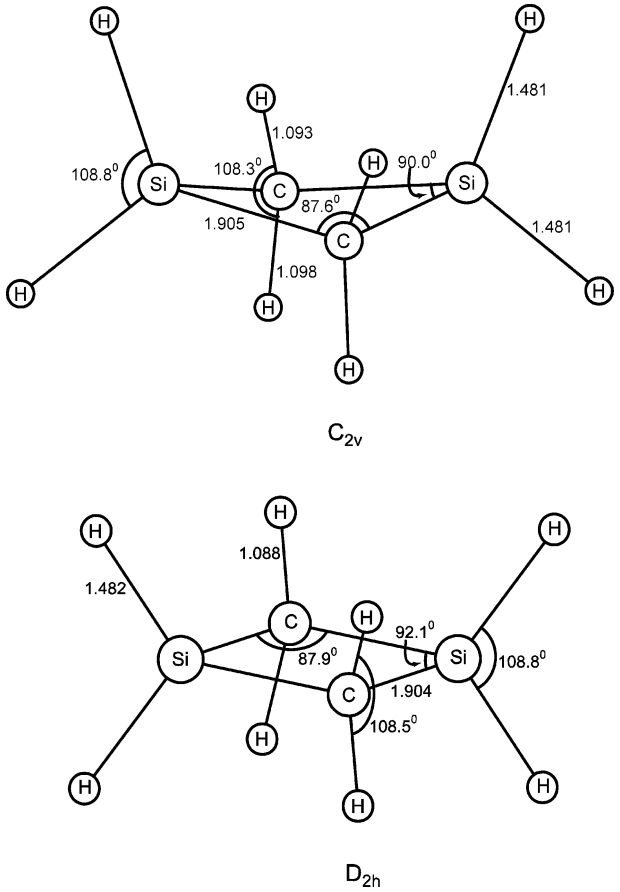


**Figure 1.** Calculated structures of puckered ($C_{2v}$) and planar ($D_{2h}$) 13DSCB.

done for the h$_4$ isotopomer since there was insufficient sample. The A, B, and C rotational constants for the $C_{2v}$ structure of the $d_4$ molecule were calculated to be 0.2223, 0.1123, and 0.08755 cm$^{-1}$, respectively, in excellent agreement with 0.2226, 0.1132, and 0.08748 cm$^{-1}$ from the microwave. While the calculated A and C constants differ by only about 0.1% from the experimental values, the 0.8% difference in the B constant reflects the small difference between the calculated and observed dihedral angles of puckering. The $I_b$ moment of inertia, which has its axis passing through the two carbon atoms for the $D_{2h}$ structure, is most affected by the value of the puckering coordinate. Table 1 also compares the bond distances and angles reported in the microwave work to calculated values from our study, and the agreement is very good.

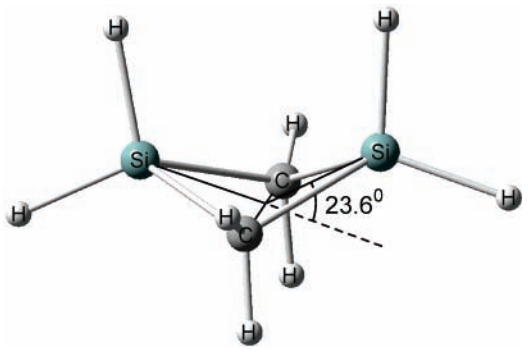


**Figure 2.** Dihedral angle of puckered 13DSCB.

A very interesting feature of the 13DSCB structure is that the CSiC angles are larger than the SiCSi angles. This was first observed in the microwave work where the CSiC angle was reported to be 92.33 ± 0.23°. The calculated value here is 90.0° and the SiCSi angle is 87.6°. This is counterintuitive, as the CSiC angle is expected to be more flexible as it has a smaller force constant. However, Kubota et al.[5] rationalize this result in terms of "bent" C−Si bonds. Another possible explanation involves the partial charges on the ring atoms. As discussed later, the carbon atoms have greater partial negative charges (−0.49) than the silicon atoms have partial positive charges (+0.35). Hence, the carbon atoms will have a tendency to push each other further apart than do the silicon atoms, thereby expanding the CSiC angles.

**Assignment of Spectra.** Figures 3 and 4 compare the calculated infrared and Raman spectra, respectively, of 13DSCB to the experimental liquid-phase spectra. The vapor-phase spectra, which are expected to give better frequency agreement, are not shown since the vapor-phase band shapes tend to disguise the intensity correlations. Figures 5 and 6 compare the calculated and experimental spectra for the 13DSCB-1,1,3,3-$d_4$ isotopomer. As can be seen for all cases, both the frequency and the intensity correlations are excellent. Tables 2 and 3 compare the calculated frequencies for both isotopomers to their experimental vapor and liquid values. Several of these have been reassigned based on both frequency and intensity correlations for the $C_{2v}$ structures. These will be discussed below in more detail. The solid-state spectra, which correspond to the $D_{2h}$ planar structure, will also be discussed later.

In order to confirm the new vibrational assignments, we examined the infrared and Raman bands which were calculated to be the most intense, and we compared these to the observed spectra for both types of spectra for both molecules. These

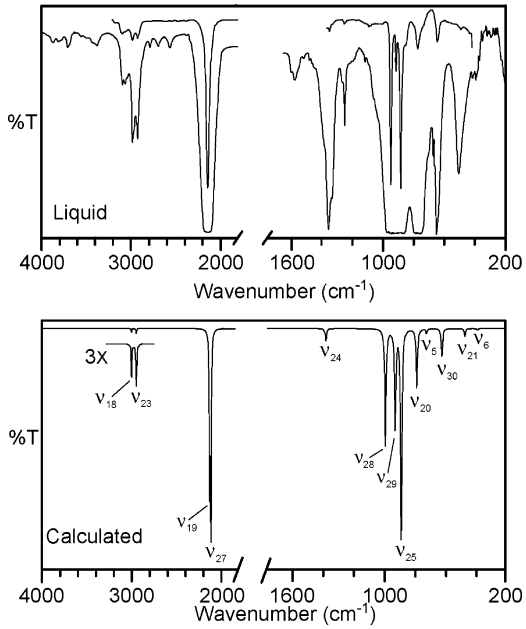


**Figure 3.** Infrared spectrum of liquid 13DSCB compared to its calculated spectrum.

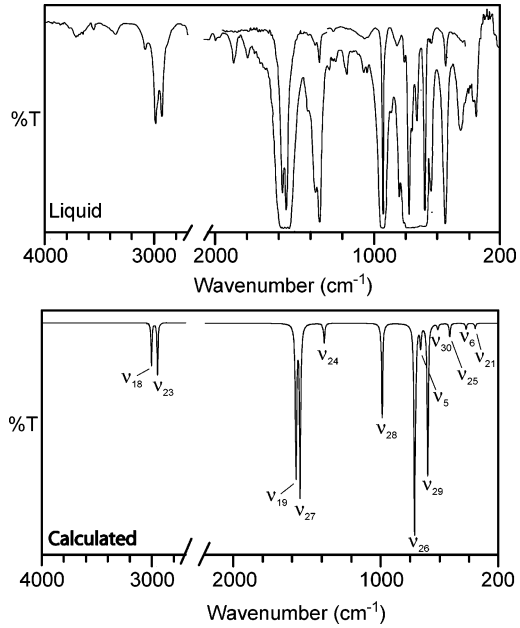


**Figure 5.** Infrared spectrum of liquid 13DSCB-$d_4$ compared to its calculated spectrum.

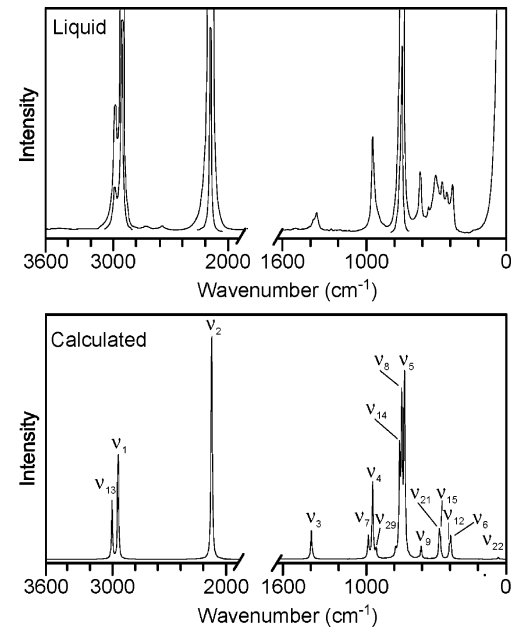


**Figure 4.** Raman spectrum of liquid 13DSCB compared to its calculated spectrum.

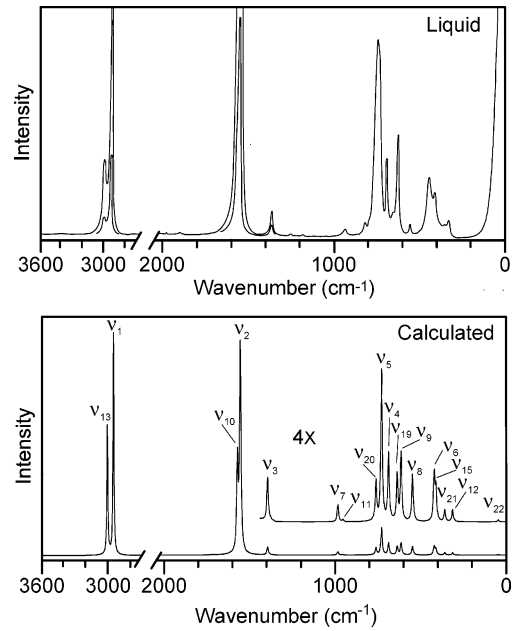


**Figure 6.** Raman spectrum of liquid 13DSCB-$d_4$ compared to its calculated spectrum.

frequencies for these bands are shown as bold numbers in Tables 2 and 3, and a remarkably good correlation can be seen. The agreement is such that every infrared and Raman band calculated to have substantial intensity in fact does appear prominently in the spectra very close to the predicted frequency value. This excellent agreement for these intense bands is especially important because, as Tables 2 and 3 show, the calculated $CH_2$ wagging and twisting frequencies, which mostly have very weak intensities, are at unexpectedly low values. Conventional wisdom places these in the 1100−1300 $cm^{-1}$ range with the wagging motions about 100 $cm^{-1}$ higher than the twists. However, 13DSCB has its calculated wags at 988 ($\nu_7$) and 996 $cm^{-1}$ ($\nu_{28}$) and the twists at 976 ($\nu_{11}$) and 935 $cm^{-1}$ ($\nu_{16}$). Except for $\nu_{28}$ observed at 965 $cm^{-1}$ for the vapor as a strong infrared band, all of these are predicted to be very weak and thus were difficult to assign without these computations. Previously,[2] the $CH_2$ wagging and twisting were assigned near 1260 and 1120 $cm^{-1}$, respectively, based on weak infrared and Raman bands. Colthup, Wiberly, and Daley[11] state that these modes in general for substituted cyclobutanes should be in the 1245−1220 $cm^{-1}$ range for the wags and 1250−1050 $cm^{-1}$ for the twists. For $SiCH_2R$ groups the wag is stated to be in the 1250−1200 $cm^{-1}$ region. On the basis of the DFT calculations, however, for 13DSCB these modes are approximately 200 $cm^{-1}$ lower, and the reason for this will be discussed later. The very weak bands near 1120 and 1260 $cm^{-1}$, previously assigned to the twists and wags, are apparently overtone or combination bands. For example, the former is likely $\nu_5 + \nu_6$ (745 + 380 = 1125 $cm^{-1}$) and the later $\nu_9 + \nu_{30}$ (620 + 644 = 1266 $cm^{-1}$). For the $d_4$ isotopomer, the wags and the twists are calculated to be at 986

**TABLE 2: Vibrational Assignment (in cm$^{-1}$) of 13DSCB-$h_4$ (Vapor and Liquid)[a]**

| symmetry | | | | vapor | | liquid | | calcd[b] |
|---|---|---|---|---|---|---|---|---|
| $D_{2h}$ | $C_{2v}$ | $n$ | approx. description | IR | Raman[c] | IR | Raman[c] | $C_{2v}$ |
| $A_g$ | $A_1$ | 1 | $CH_2$ sym. str. (ip) | 2930 w | **2931 (100)** | (2920) | **2923 (20)** | 2951 (4, 626) |
| | | 2 | $SiH_2$ sym. str. (ip) | **2155 s** | **2156 (1000)** | (2169) | **2148 (1000)** | 2125 (140, 1000) |
| | | 3 | $CH_2$ deform (ip) | | **1373 (2)** | 1355 mw | **1355 (5)** | 1396 (4, 18) |
| | | 4 | $SiH_2$ deform (ip) | (965) | **965 (11)** | | **958 (32)** | 956 (7, 47) |
| | | 5 | ring breathing | **745 m** | **745 (134)** | **742 m** | **749 (311)** | 728 (22, 109) |
| | | 6 | ring deform | 380 mw | **380 (47)** | | **385 (16)** | 397 (8, 13) |
| $B_{1g}$ | $A_2$ | 7 | $CH_2$ wag (op) | | (965) | (950) | (958) | 988 (0, 13) |
| | | 8 | $SiH_2$ wag (op) | (745) | (745) | (742) | (760) | 747 (0, 91) |
| | | 9 | ring mode | | **620 (3)** | | **617 (15)** | 609 (0, 8) |
| $B_{2g}$ | $B_1$ | 10 | $SiH_2$ antisym. str. (op) | (2155) | (2156) | (2169) | (2148) | 2129 (10, 450) |
| | | 11 | $CH_2$ twist (ip) | (965) | (965) | (950) | (958) | 976 (9, 1) |
| | | 12 | $SiH_2$ rock (op) | (380) | (380) | | **429 (10)** | 406 (0.4, 6) |
| $B_{3g}$ | $B_2$ | 13 | $CH_2$ antisym. str. (op) | 2995 w | **2989 (10)** | (2980) | **2981 (44)** | 3004 (7, 287) |
| | | 14 | $CH_2$ rock (op)[d] | (745) | (745) | (775) | **760 (50)** | 762 (2, 61) |
| | | 15 | $SiH_2$ twist (ip)[d] | 442 mw | **442 (3)** | (440) | **460 (10)** | 469 (1, 10) |
| $A_u$ | $A_2$ | 16 | $CH_2$ twist ((op) | | | (918) | (928) | 935 (0, 0.1) |
| | | 17 | $SiH_2$ twist (op) | | | | 555 (3) | 571 (0, 0.2) |
| $B_{1u}$ | $A_1$ | 18 | $CH_2$ antisym. str. (ip) | **2965 m** | 2950 (52) | **2980 w** | (2981) | 3003 (13, 90) |
| | | 19 | $SiH_2$ antisym. str. (ip) | **2157 vvs** | (2156) | **2169 vvs** | (2148) | 2133 (709, 311) |
| | | 20 | $CH_2$ rock (ip)[d] | **∼780 ms** | | **775 m** | (760) | 792 (293, 4) |
| | | 21 | $SiH_2$ rock (ip)[d] | **438 mw** | 446 (13) | **∼440 vw** | (460) | 478 (38, 16) |
| | | 22 | ring puckering | 56 | 56 | | | 54 (7, 1) |
| $B_{2u}$ | $B_2$ | 23 | $CH_2$ sym. str. (op) | **2930 w** | (2931) | **2920 w** | (2923) | 2950 (21, 23) |
| | | 24 | $CH_2$ deform (op) | **1363 mw** | (1373) | **1330 mw** | | 1384 (62, 1) |
| | | 25 | $SiH_2$ wag (ip) | **905 s** | 905 (1) | **886 vs** | 875 (1) | 893 (1000, 0) |
| | | 26 | ring mode | (644) | (620) | | (617) | 636 (6, 0.2) |
| $B_{3u}$ | $B_1$ | 27 | $SiH_2$ sym. str. (op) | **2147 vvs** | 2147 (44) | (2169) | (2148) | 2117 (933, 48) |
| | | 28 | $CH_2$ wag (ip) | **965 s** | (965) | **950 vs** | (958) | 996 (561, 0.1) |
| | | 29 | $SiH_2$ deform (op) | **928 m** | | **918 m** | 928 (5) | 931 (493, 5) |
| | | 30 | ring mode | **644 m** | | **650 m** | | 627 (135, 0.5) |

[a] w, weak; m, medium; s, strong; v, very; ip, in-phase, op, out-of-phase. The intensities of frequencies in parentheses result primarily from another vibration at that frequency. [b] Frequencies were calculated using B3LYP/6-311++G(d,p) level of theory, and the values in the parentheses are the calculated relative IR and Raman intensities respectively. [c] Values in the parentheses are relative Raman intensities. [d] These vibrational modes next to each other are strongly coupled.

**TABLE 3: Vibrational Asignment (in cm$^{-1}$) of 13DSCB-$d_4$ (Vapor and Liquid)[a]**

| symmetry | | | | vapor | | liquid | | calcd[b] |
|---|---|---|---|---|---|---|---|---|
| $D_{2h}$ | $C_{2v}$ | $n$ | approx. description | IR | Raman[c] | IR | Raman[c] | $C_{2v}$ |
| $A_g$ | $A_1$ | 1 | $CH_2$ sym. str. (ip) | (2930) | **2920 (53)** | (2925) | **2925 (37)** | 2950 (0.6, 100) |
| | | 2 | $SiD_2$ sym. str. (ip) | (1554) | **1554 (100)** | (1549) | **1555 (100)** | 1556 (0, 97) |
| | | 3 | $CH_2$ deform (ip) | | **1370 (3)** | 1368 vw | **1363 (3)** | 1396 (0.6, 4) |
| | | 4 | $SiD_2$ deform (ip) | (692) | **695 (20)** | (678) | **695 (7)** | 689 (0.1, 6) |
| | | 5 | ring breathing | | **754 (65)** | **730 m** | **750 (22)** | 730 (11, 13) |
| | | 6 | ring deform | 441 vw | **439 (23)** | ∼420 vw | **445 (12)** | 423 (3, 4) |
| $B_{1g}$ | $A_2$ | 7 | $CH_2$ wag (op) | | 940 (2) | (940) | 940 (1) | 986 (0, 1) |
| | | 8 | $SiD_2$ wag (op) | | 546 (1) | | 555 (2) | 549 (0, 4) |
| | | 9 | ring mode | | **620 (7)** | | (629) | 616 (0, 6) |
| $B_{2g}$ | $B_1$ | 10 | $SiD_2$ antisym. str. (op) | (1576) | **1579 (74)** | (1575) | **1568 (50)** | 1573 (0.5, 39) |
| | | 11 | $CH_2$ twist (ip) | | (940) | | (940) | 956 (0.01, 0.2) |
| | | 12 | $SiD_2$ rock (op) | | 332(2) | 352 w | 330(2 ) | 315 (0.02, 1) |
| $B_{3g}$ | $B_2$ | 13 | $CH_2$ antisym. str. (op) | 2972 vvw | **2974 (4)** | (2982) | **2985 (11)** | 3004 (1, 46) |
| | | 14 | $CH_2$ rock (op)[d] | | **635 (7)** | (640) | **629 (12)** | 639 (0, 4) |
| | | 15 | $SiD_2$ twist (ip)[d] | | **428 (6)** | (420) | **411 (4)** | 412 (0.03, 3) |
| $A_u$ | $A_2$ | 16 | $CH_2$ twist ((op) | | | | | 894 (0, 0) |
| | | 17 | $SiD_2$ twist (op) | | (428) | 450 mw? | (411) | 425 (0, 0.1) |
| $B_{1u}$ | $A_1$ | 18 | $CH_2$ antisym. str. (ip) | **2950 vvw** | 2941 (24) | **2982 mw** | (2985 ) | 3003 (2, 15) |
| | | 19 | $SiD_2$ antisym. str. (ip) | **1576 vvs** | 1574 (17) | **1575 vvs** | (1568 ) | 1575 (75, 4) |
| | | 20 | $CH_2$ rock (ip)[d] | (791) | 795 (1) | (780) | 792 (1) | 763 (22, 3) |
| | | 21 | $SiD_2$ rock (ip)[d] | **344 vw** | 344 (4) | **360 vw** | 360 (1) | 361 (3, 1) |
| | | 22 | ring puckering | 52 | 52 | | | 48 (1, 0.1)) |
| $B_{2u}$ | $B_2$ | 23 | $CH_2$ sym. str. (op) | **2930 vw** | (2920) | **2925 mw** | (2925 ) | 2950 (3, 4) |
| | | 24 | $CH_2$ deform (op) | **1339 m** | | **1340 mw** | | 1384 (10, 0.2) |
| | | 25 | $SiD_2$ wag (ip) | **543 m** | (546) | **548 m** | (555) | 533 (7, 0.02) |
| | | 26 | ring mode | **791 vvw** | (795) | **780 s** | (792) | 771 (100, 0.1) |
| $B_{3u}$ | $B_1$ | 27 | $SiD_2$ sym. str. (op) | **1554 vvs** | 1556 (15) | **1549 vvs** | (1555 ) | 1548 (86, 1) |
| | | 28 | $CH_2$ wag (ip) | **951 vvs** | | **943 s** | (940) | |
| | | 29 | $SiD_2$ deform (op) | **692 vvs** | 685 (4) | **678 s** | | |
| | | 30 | ring mode | **629 m** | (620) | **640 m** | (629) | |

[a] See the footnote of Table 2 for abbreviations.

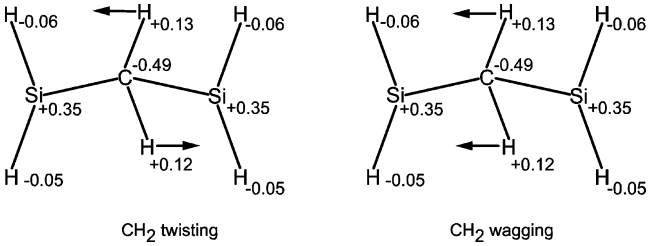


**Figure 7.** $SiH_2$ twisting and wagging vibrations of 13DSCB and the partial charges calculated for each atom from the B3LYP/6-311++G(d,p) calculation. The attraction between unlike charges lowers the frequencies of these two vibrational modes.

**TABLE 4: Vibrational Assignment (in $cm^{-1}$) of 13DSCB-$h_4$ (solid)[a]**

| symmetry | | | solid | | calcd[b] |
|---|---|---|---|---|---|
| $D_{2h}$ | $\nu$ | approx. description | IR | Raman[c] | $D_{2h}$ |
| $A_g$ | 1 | $CH_2$ sym. str. (ip) | (2925) | **2918 (199)** | 2954 (0, 531) |
| | 2 | $SiH_2$ sym. str. (ip) | (2140) | **2146 (1000)** | 2124 (0, 1000) |
| | 3 | $CH_2$ deform (ip) | 1360 m | **1349 (11)** | 1395 (0, 14) |
| | 4 | $SiH_2$ deform (ip) | (955) | **949 (42)** | 955 (0, 41) |
| | 5 | ring breathing | | **740 (500)** | 725 (0, 92) |
| | 6 | ring angle bending | 419 vw | **422 (65)** | 417 (0, 19) |
| $B_{1g}$ | 7 | $CH_2$ wag (op) | (955) | (949) | 989 (0, 11) |
| | 8 | $SiH_2$ wag (op) | (768) | **767 (75)** | 754 (0, 75) |
| | 9 | ring mode | | **607 (6)** | 608 (0, 6) |
| $B_{2g}$ | 10 | $SiH_2$ antisym. str. (op) | (2140) | **2156 (55)** | 2126 (0, 430) |
| | 11 | $CH_2$ twist (ip) | (955) | (949) | 974 (0, 1) |
| | 12 | $SiH_2$ rock (op) | | (422) | 401 (0, 6) |
| $B_{3g}$ | 13 | $CH_2$ antisym. str. (op) | (2968) | **2971 (97)** | 3001 (0, 266) |
| | 14 | $CH_2$ rock (op)[d] | | (767) | 762 (0, 51) |
| | 15 | $SiH_2$ twist (ip)[d] | (465) | **450 (11)** | 468 (0, 7) |
| $A_u$ | 16 | $CH_2$ twist ((op) | (928) | | 933 (0, 0) |
| | 1 | $SiH_2$ twist (op) | | 562 (1) | 578 (0, 0) |
| $B_{1u}$ | 18 | $CH_2$ antisym. str. (ip) | **2968 w** | 2962 (62) | 3000 (16, 0) |
| | 19 | $SiH_2$ antisym. str. (ip) | (2140) | 2162 (8) | 2128 (852, 0) |
| | 20 | $CH_2$ rock (ip)[d] | **768 s** | (767) | 786 (309, 0) |
| | 21 | $SiH_2$ rock (ip)[d] | **465 w** | 465 (17) | 457 (47, 0) |
| | 22 | ring puckering | - | - | i |
| $B_{2u}$ | 23 | $CH_2$ sym. str. (op) | **2925 w** | 2920 (146) | 2954 (25, 0) |
| | 24 | $CH_2$ def (op) | **1338 m** | (1349) | 1383 (67, 0) |
| | 25 | $SiH_2$ wag (ip) | **880 vs** | 875 (1) | 895 (1000, 0) |
| | 26 | ring mode | (650) | 617 (85) ? | 637 (8, 0) |
| $B_{3u}$ | 27 | $SiH_2$ sym. str. (op) | **2140 vvs** | 2140 (200) | 2115 (920, 0) |
| | 28 | $CH_2$ wag (ip) | **955 vs** | | 994 (585, 0) |
| | 29 | $SiH_2$ deform (op) | **928 s** | 927 (4) | 931 (465, 0) |
| | 30 | ring mode | **650 s** | 646 (1) | 627 (136, 0) |

[a] See the footnote of Table 2 for abbreviations.

($\nu_7$), 991 ($\nu_{28}$), 956 ($\nu_{11}$), and 894 $cm^{-1}$ ($\nu_{16}$), respectively. Again, all but $\nu_{28,}$ which is a very strong band in the infrared at 951, are predicted to have negligible intensity.

**Anomalous $CH_2$ Wagging and Twisting Frequencies.** As mentioned above, the $CH_2$ wagging frequencies for the $h_4$ molecule of 988 ($\nu_7$ calculated) and 965 ($\nu_{28}$) $cm^{-1}$ and the twisting frequencies of 976 ($\nu_{11}$ calculated) and 935 ($\nu_{16}$ calculated) are far below those typically observed. Notably, the $CH_2$ deformations at 1373 ($\nu_3$) and 1363 ($\nu_{24}$) $cm^{-1}$ and the $CH_2$ rocks at 760 ($\nu_{15}$) and 780 ($\nu_{20}$) are not outside their normal ranges. The anomalous wagging and twisting frequencies can be understood by considering the partial changes on the hydrogen atoms attached to the carbon and silicon atoms, as shown in Figure 7. The carbon hydrogens have positive partial charges while those on silicon are negatively charged due to the electropositive nature of the silicon atoms. The values for the charges in the figure are from the ab initio calculations. The sideways motions of the positively charged carbon hydrogen atoms during a twisting or wagging motion brings them closer to the negatively charged hydrogens on the silicon atoms. Hence, this attraction between opposite charges counteracts the usual increase in potential energy away from the equilibrium positions of the $CH_2$ groups. The steepness of the potential energy curve is thus decreased and lower vibrational frequencies result. A previous study,[12] which was carried out at the SCF level, suggested that decreased frequencies for these types of modes might result, but here we see very clear evidence for these unprecedented low values. The previous study also did not calculate any Raman intensities so the correlations with the experimental spectra were not easily done. Nonetheless, the values previously calculated for the most part are within 15 $cm^{-1}$ of our values presented here, although some of the CH and SiH stretching frequencies differ by 40 $cm^{-1}$ or more.

**TABLE 5: Vibrational Assignment (in $cm^{-1}$) of 13DSCB-$d_4$ (Solid)[a]**

| symmetry | | | solid | | calcd[b] |
|---|---|---|---|---|---|
| $D_{2h}$ | $\nu$ | approx. description | IR | Raman[c] | $D_{2h}$ |
| $A_g$ | 1 | $CH_2$ sym. str. (ip) | (2920) | 2920 (63) | 2954 (0, 100) |
| | 2 | $SiD_2$ sym. str. (ip) | (1549) | **1555 (100)** | 1554 (0, 91) |
| | 3 | $CH_2$ deform (ip) | 1357 m | **1355 (8)** | 1394 (0, 3) |
| | 4 | $SiD_2$ deform (ip) | (672) | **688 (15)** | 689 (0, 6) |
| | 5 | ring breathing | (740) | **740 (101)** | 733 (0, 15) |
| | 6 | ring angle bending | | **406 (25)** | 400 (0, 4) |
| $B_{1g}$ | 7 | $CH_2$ wag (op) | (940) | (945) | 987 (0, 1) |
| | 8 | $SiD_2$ wag (op) | (560) | 555 (1) | 553 (0, 4) |
| | 9 | ring mode | | **617 (6)** | 619 (0, 6) |
| $B_{2g}$ | 10 | $SiD_2$ antisym. str. (op) | (1570) | **1564 (56)** | 1570 (0, 40) |
| | 11 | $CH_2$ twist (ip) | (940) | 945 (2) | 953 (0, 0.2) |
| | 12 | $SiD_2$ rock (op) | 353 vw | **350 (2)** | 311 (0, 1) |
| $B_{3g}$ | 13 | $CH_2$ antisym. str. (op) | (2960) | **2974 (56)** | 3001 (0, 50) |
| | 14 | $CH_2$ rock (op)[d] | | **638 (59)** | 635 (0, 4) |
| | 15 | $SiD_2$ twist (ip)[d] | 420 vw | **419 (12)** | 413 (0, 2) |
| $A_u$ | 16 | $CH_2$ twist (op) | | | 891(0, 0) |
| | 17 | $SiD_2$ twist (op) | 450 mw | 454 (2) | 429 (0, 0) |
| $B_{1u}$ | 18 | $CH_2$ antisym. str. (ip) | **2960 m** | 2962 (19) | 3000 (2, 0) |
| | 19 | $SiD_2$ antisym. str. (ip) | **1570 vs** | 1574 (13) | 1573 (75, 0) |
| | 20 | $CH_2$ rock (ip)[d] | 740 m | (740) | 751 (31, 0) |
| | 21 | $SiD_2$ rock (ip) [d] | **381 mw** | (406) | 383 (6, 0) |
| | 22 | ring puckering | | | i |
| $B_{2u}$ | 23 | $CH_2$ sym. Str. (op) | **2920 m** | 2925 (41) | 2954 (4, 0) |
| | 24 | $CH_2$ deform (op) | **1326 m** | | 1383 (10, 0) |
| | 25 | $SiD_2$ wag (ip) | **560 ms** | (555) | 535 (6, 0) |
| | 26 | ring mode | **772 s** | | 770 (100, 0) |
| $B_{3u}$ | 27 | $SiD_2$ sym. str. (op) | **1549 vs** | | 1546 (84, 0) |
| | 28 | $CH_2$ wag (ip) | **940 s** | (945) | 989 (47, 0) |
| | 29 | $SiD_2$ deform (op) | **672 s** | (688) | 683 (75, 0) |
| | 30 | ring mode | **640 m** | | 614 (3, 0) |

[a] See the footnote of Table 2 for abbreviations.

**Structural Conversion in the Solid Phase.** As we postulated previously, 13DSCB converts from $C_{2v}$ symmetry (puckered) to $D_{2h}$ (planar) in the solid phase. Tables 4 and 5 compare the calculated $D_{2h}$ frequencies to those of solid 13DSCB-$h_4$ and -$d_4$. Since the vapor-phase structure for the independent molecule is not planar, the calculated ring-puckering frequency is imaginary.

Figure 8 shows the Raman spectra of the vapor, liquid, and solid 12DSCB-$h_4$ and -$d_4$ in the low-frequency region. The dramatic change in $\nu_6$, the ring angle bending, from 380, to 385, to 422 $cm^{-1}$ in going from the vapor, to liquid, to solid phases can be seen. For the -$d_4$ molecule, the corresponding values are 441, 445, and 406 $cm^{-1}$. At the same time $\nu_{21}$, the $SiH_2$ in-phase rocking, has values of 436 (vapor), 440 (liquid, from the infrared), and 465 $cm^{-1}$ (solid) for 13DSCB-$h_4$ and 344, 360, and 381 $cm^{-1}$ (solid) for the -$d_4$ isotopomer. The large change in the frequencies for the solid results from the fact that $\nu_6$ and $\nu_{21}$ are now of different symmetry species ($A_g$ and $B_{1u}$)

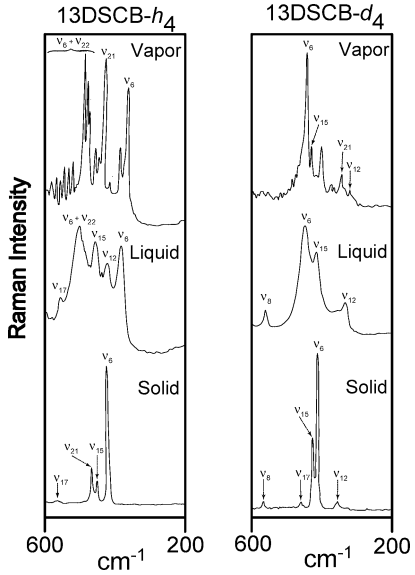


**Figure 8.** Raman spectra of 13DSCB-$h_4$ and -$d_4$ for its vapor, liquid, and solid (77 K) in the 200−600 cm$^{-1}$ region.

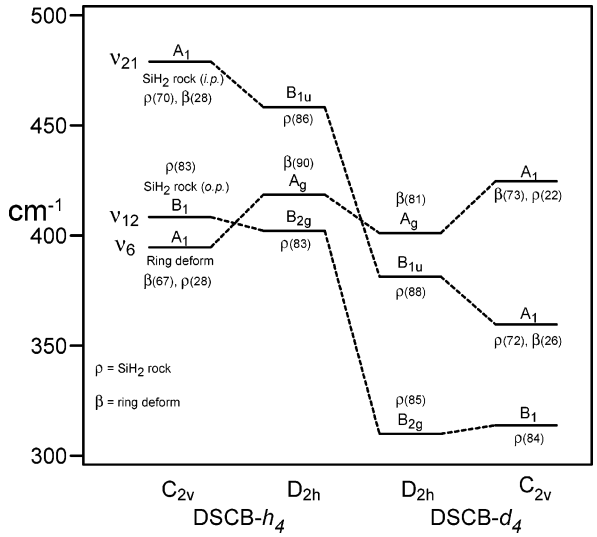


**Figure 9.** Correlation diagram for $\nu_6$ (ring-angle bending), $\nu_{12}$ ($SiH_2$ out-of-phase rocking), and $\nu_{21}$ ($SiH_2$ in-phase rocking) for DSCB-$h_4$ and -$d_4$ for their $C_{2v}$ (puckered vapor) and $D_{2h}$ (planar solid) structures. For $C_{2v}$ symmetry, $\nu_6$ and $\nu_{21}$ interact; for $D_{2h}$, they do not. $\beta$ and $\rho$ indicate the percent potential energy distribution from the ring bending and $SiH_2$ rocking modes respectively.

and can no longer interact as their motions are orthogonal. In the puckered $C_{2v}$ structure both vibrations are of $A_1$ symmetry species and the up and down motion of the $SiH_2$ rocking can easily interact with the angle bendings which now have a component perpendicular to the original plane of the molecule. This is all depicted in Figure 9, where the calculated frequencies for both isotopomers are shown for $C_{2v}$ and $D_{2h}$ symmetries. For $D_{2h}$ the $A_g$ ($\nu_6$) and $B_{1u}$ ($\nu_{21}$) modes have similar frequencies for both isotopomers, but they are pushed apart for the $C_{2v}$ (vapor) cases. In the vapor phase, the potential energy distribution for $\nu_{21}$ at 436 cm$^{-1}$ is 0.70 $SiH_2$ rock and 0.28 angle bending, while $\nu_6$ is 0.67 bending and 0.28 rock for the $h_4$ isotopomer. For the planar solid, $\nu_{21}$ and $\nu_6$ are almost purely the rock and bend, respectively. These values are shown in the figure. Similarly, for the $d_4$ isotopomer, $\nu_6$ is 0.73 bending, 0.22 rocking, while $\nu_{21}$ is 0.72 rocking and 0.26 bending. The vibrations again become nearly "pure" for the planar $D_{2h}$ form. It is very reassuring that our assessment in 1977, based on force constant calculations, was just the same, and now we have reconfirmation of the phase-dependent structure of 13DSCB. It should be added that we are aware of no other type of analysis that could have been used to ascertain the structure and symmetry changes of this molecule in the solid since it would not have been possible to grow crystals of the molecule at low temperatures for crystallography studies.

## Conclusion

13DSCB is a very remarkable molecule. It has apparently only been prepared in our laboratory and that was three decades ago. It has several highly unusual features. First, the CSiC angles are larger than the SiCSi angles although the force constant for the former is typically much smaller, and therefore these angles should be able to accommodate the angle strain in the ring to a greater extent. This is not the case, however, possibly because of charge repulsions across the four-membered ring. Second, the $CH_2$ wagging and twisting frequencies for 13DSCB are the lowest by far of any that we are aware of. This results from charge attractions between neighboring hydrogen atoms. In the near future, we will provide further evidence for this effect in other cyclic silanes. However, for 13DSCB, it is the most dramatic. The third unusual feature of 13DSCB is its change in structure in the solid phase. The DFT calculations beautifully confirm our earlier conclusions about the changes in vibrational coupling. The structural change itself is not so surprising as planar 13DSCB molecules can obviously stack together better in the solid than can puckered ones. Since the energy barrier between the $C_{2v}$ and the $D_{2h}$ is so small (0.25 kcal/mol) for the individual molecules in the vapor, even tiny intermolecular interactions in the solid phase can easily overcome this energy difference between the two conformations. The effect on the spectra, however, has been very substantial.

**Acknowledgment.** The authors wish to thank the National Science Foundation (Grant CHE-0131935) and the Robert A. Welch Foundation (Grant A-0396) for financial support.

## References and Notes

(1) Irwin, R. M.; Cooke, J. M.; Laane, J. *J. Am. Chem. Soc.* **1977**, *99*, 3273.

(2) Irwin, R. M.; Laane J. *J. Phys. Chem.* **1978**, *82*, 2845.

(3) Kubota, T.; Ueda, K.; Tanaka, T.; Laane, J. *J. Mol. Spectrosc.* **1988**, *128*, 250.

(4) Kubota, T.; Ueda, K.; Tanaka, T.; Laane, J. *J. Mol. Spectrosc.* **1985**, *114*, 234.

(5) Irwin, R. M. Ph.D. Thesis, Texas A&M University, College Station, TX, 1978.

(6) Frisch, M. J.; Trucks, G. W.; Schlegel, H. B.; Scuseria, G. E.; Robb, M. A.; Cheeseman, J. R.; Montgomery, J. A., Jr.; Vreven, T.; Kudin, K. N.; Burant, J. C.; Millam, J. M.; Iyengar, S. S.; Tomasi, J.; Barone, V.; Mennucci, B.; Cossi, M.; Scalmani, G.; Rega, N.; Petersson, G. A.; Nakatsuji, H.; Hada, M.; Ehara, M.; Toyota, K.; Fukuda, R.; Hasegawa, J.; Ishida, M.; Nakajima, T.; Honda, Y.; Kitao, O.; Nakai, H.; Klene, M.; Li, X.; Knox, J. E.; Hratchian, H. P.; Cross, J. B.; Bakken, V.; Adamo, C.; Jaramillo, J.; Gomperts, R.; Stratmann, R. E.; Yazyev, O.; Austin, A. J.; Cammi, R.; Pomelli, C.; Ochterski, J. W.; Ayala, P. Y.; Morokuma, K.; Voth, G. A.; Salvador, P.; Dannenberg, J. J.; Zakrzewski, V. G.; Dapprich, S.; Daniels, A. D.; Strain, M. C.; Farkas, O.; Malick, D. K.; Rabuck, A. D.; Raghavachari, K.; Foresman, J. B.; Ortiz, J. V.; Cui, Q.; Baboul, A. G.; Clifford, S.; Cioslowski, J.; Stefanov, B. B.; Liu, G.; Liashenko, A.; Piskorz, P.; Komaromi, I.; Martin, R. L.; Fox, D. J.; Keith, T.; Al-Laham, M. A.; Peng, C. Y.; Nanayakkara, A.; Challacombe, M.; Gill, P. M. W.; Johnson, B.; Chen, W.; Wong, M. W.; Gonzalez, C.; Pople, J. A. Gaussian *03*, Revision C.02; Gaussian, Inc.: Wallingford CT, 2004.

(7) Yang, J.; McCann, K.; Laane, J. *J. Mol. Struc.* **2004**, *339*, 695−696.

(8) Autrey, D.; Yang, J.; Laane, J. *J. Mol. Struc.* **2003**, *23*, 661−662.
(9) Autrey, D.; Arp, Z.; Choo, J.; Laane, J. *J. Chem. Phys.* **2003**, *119*, 2557.
(10) Autrey, D.; Haller, K.; Laane, J.; Mlynek, C.; Hopf, H. *J. Phys. Chem. A* **2004**, *108*, 403.
(11) Lin-Vien, D.; Colthup, N. B.; Fateley, W. G.; Grasselli, J. G.; *Infrared and Raman Characteristic Frequencies of Organic Molecules*; Academic Press: San Diego, CA, 1991; pp 23 and 257.
(12) Seidl, E. T.; Grev, R. S.; Schaefer, H. F., III *J. Am. Chem. Soc.* **1992**, *114*, 3643.